Journal of Alloys and Compounds 516 (2012) 157–160

Contents lists available at SciVerse ScienceDirect

Journal of Alloys and Compounds

journal homepage: www.elsevier.com/locate/jallcom

Preparation and properties of p-type Ag-doped ZnMgO thin films by pulsed laser deposition

Ling Cao, Liping Zhu*, Jie Jiang, Yang Li, Yinzhu Zhang, Zhizhen Ye

State Key Laboratory of Silicon Materials, Department of Materials Science and Engineering, Zhejiang University, Hangzhou 310027, People's Republic of China

ARTICLE INFO

Article history:
Received 17 October 2011
Received in revised form 5 December 2011
Accepted 6 December 2011
Available online 16 December 2011

Keywords:
Semiconductors
Thin films
Pulsed laser deposition
Optical properties
Scanning electron microscopy

ABSTRACT

We report on p-type Ag-doped ZnMgO thin films prepared on quartz substrates by pulsed laser deposition. The effects of substrate temperature on the structural, electrical and optical properties of the films are investigated in detail. All the films we obtained have a preferred orientation with the *c*-axis perpendicular to the substrates. Secondary ion mass spectroscopy and X-ray photoelectron spectroscopy measurements confirm that Ag has been incorporated into the films and principally occupies Zn site in the state of Ag^+ ion and acts as an acceptor. An acceptable p-type conduction, with a resistivity of 24.96 Ω cm, a Hall mobility of 0.32 $cm^2 V^{-1} s^{-1}$, and a hole concentration of 7.89×10^{17} cm^{-3} at room temperature, was obtained for the film grown at the optimal substrate temperature of 400 °C. The formation of good p-type conduction in this film might be due to a combined effect of the increase of substitutional-Ag (Ag_{Zn}) density and the suppression of the oxygen-related defects. The p-type conduction of Ag-doped ZnMgO film is further confirmed by a rectifying Ag-doped ZnMgO/i-ZnO/Al-doped ZnMgO heterojunction.

1. Introduction

Zinc oxide (ZnO), with a direct band gap of 3.37 eV at room temperature and a high exciton binding energy of 60 meV, has attracted great attention in recent years due to its promising potential applications in blue and ultraviolet (UV) light-emitting diodes (LEDs) and laser diodes (LDs) [1,2]. It is well known that the band gap of ZnO can be modulated by alloying different concentrations of MgO [3]. Therefore, ZnMgO is a suitable material for ZnO/ZnMgO superlattices, quantum wells, and ultraviolet (UV) optoelectronic devices [4]. On the other hand, the p-n junction based on ZnMgO not only improves the efficiency of UV or blue light emitting devices even working at deep UV wavebands, but also results in new application opportunities such as laser diodes in message storage [5]. In order to realize such optoelectronic application, it is necessary to obtain high-quality, reproducible, and stable n-type and p-type doping. The n-type ZnMgO thin films with high crystal quality can far more readily be prepared even without any doping [6]. However, as in ZnO, fabrication of p-type ZnMgO thin films with high optical quality and stable conductivity is still very difficult due to the low dopant solubility, the deep acceptor levels of the dopants, and the self-compensation effect from native defects such as oxygen vacancy (V_O) and zinc interstitial (Zn_i) [7]. Therefore, many attempts have been made to obtain p-type ZnMgO thin films by single doping of I or V group elements, such as Li [8], Na [9], N [10], P [11], As [12], Sb [13], etc., and codoping of III–V groups, such as, Al–N [14], etc. Recently, realization of p-type ZnMgO with K-doping and In–N co-doping prepared by pulsed laser deposition and direct current magnetron sputtering, respectively, have been reported [15,16]. Besides these abovementioned acceptor dopants, Ag, as a group IB element, is a good candidate for producing a shallow acceptor level in ZnO under oxygen-rich growth conditions, if incorporated on substitutional Zn sites [17,18]. The first-principles calculations demonstrated that the formation energy of Ag_{Zn} is much lower than that of Ag_i, thus the compensation effects of the interstitial atoms can be restrained strongly. In addition, the O-rich conditions likely needed to prevent compensating V_O and/or Zn_i defects are consistent with the required conductions for substituting Ag onto the Zn sites. However, there is no report, to the best of our knowledge, on the formation of p-type ZnMgO thin films with Ag doping by pulsed laser deposition.

In the present study, Ag-doped ZnMgO thin films were grown on quartz substrates by pulsed laser deposition in oxygen ambient using the sintered ZnO target containing 10 at% MgO and 0.5 at% Ag_2O. The effects of substrate temperature on the structural, electrical and optical properties of the films were investigated and discussed in detail. The p-type conduction of Ag-doped ZnMgO film was further confirmed by a rectifying Ag-doped ZnMgO/i-ZnO/Al-doped ZnMgO heterojunction.

2. Experimental details

Ag-doped ZnMgO thin films were grown on quartz substrates by pulsed laser deposition in oxygen ambient. Ag-doped ZnMgO target was fabricated using high-purity ZnO (99.99%) and MgO (99.99%), with Ag_2O (99.995%) serving as the

* Corresponding author. Tel.: +86 571 87953139; fax: +86 571 87952625.
E-mail addresses: zlp1@zju.edu.cn, zjuzlp@163.com (L. Zhu).

0925-8388/$ – see front matter.
doi:10.1016/j.jallcom.2011.12.013

doping agent. The nominal concentrations of Mg and Ag in the target were 10 at% and 1 at%, respectively. A KrF excimer laser (Compex 102, 248 nm, 25 ns) was employed as the ablation source. The laser repetition rate and the energy per pulse were 5 Hz and 300 mJ, respectively. The vacuum chamber was evacuated to a base pressure of 8×10^{-4} Pa. Before being loaded into the chamber, the substrates were ultrasonically cleaned with acetone, ethanol and de-ionized water for 15 min, respectively, and subsequently dried in a flowing nitrogen gas. The deposition was carried out in high purity (99.9995%) oxygen ambient and the oxygen pressure was maintained at 45 Pa. Before deposition, the target was pre-sputtered for about 10 min to remove contaminants from the surface. The target to substrate distance was 5.5 cm and the substrate temperature was varied from 300 to 500 °C. All the films had an approximate film thickness of 280 nm. After growth, the samples were in situ annealed in a 100 Pa O_2 ambient for 30 min to suppress the formation of possible native donor defects.

The crystal structure of the films was characterized by X-ray diffraction (XRD) using a XPERT-PRO system with a Cu Kα (λ = 1.5406 Å) source. The film thickness was measured using field emission scanning electron microscopy (FE-SEM; HITACHIS-4800). The depth profile of the films was investigated by secondary ion mass spectroscopy (SIMS) (Cameca IMS-6F). The chemical bonding states of Ag was analyzed by x-ray photoelectron spectroscopy (XPS) (Thermo ESCALAB 250, Al Kα radiation source $h\nu$ = 1486.6 eV). The electrical properties were examined by Hall measurements in the van der Pauw configuration (BIO-RAD HL5500PC) at room temperature. Photoluminescence (PL) measurements were performed on a FLSP920 (Edinburgh Instruments) fluorescence spectrometer at room temperature using a He–Cd laser as a light source at excitation wavelength of 325 nm. The Ag-doped ZnMgO/i-ZnO/Al-doped ZnMgO heterojunction was made by layer-by-layer growth and the current–voltage (I–V) characteristics were evaluated by using an Agilent E5270B system.

3. Results and discussion

Fig. 1(a) shows the XRD patterns of Ag-doped ZnMgO thin films deposited at various substrate temperatures in the range of 300–500 °C. Only the peaks indexed to (0 0 2) and (0 0 4) reflections of the hexagonal wurtzite structure of ZnO can be observed in these patterns, indicating that all of the obtained films are polycrystalline

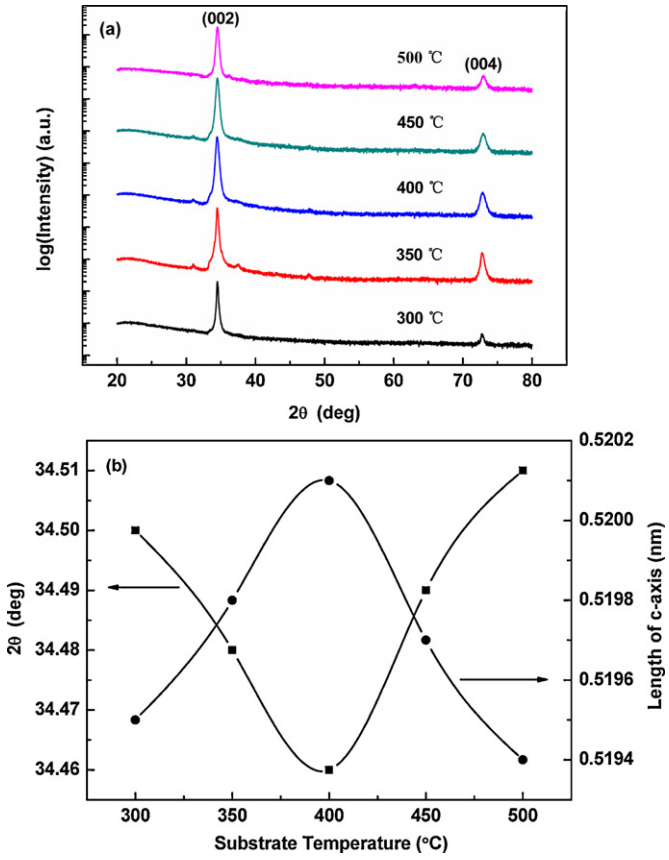

Fig. 1. (a) XRD patterns of Ag-doped ZnMgO thin films deposited at various substrate temperatures and (b) plot of substrate temperature vs (0 0 2) diffraction peak position and length of c-axis.

and have a preferred orientation with the c-axis perpendicular to the substrate surface. No extra phases related with silver oxide (Ag_2O, AgO) and/or other zinc and silver compound were detected from the XRD patterns. The (0 0 2) peak position and c-axis lattice parameter of Ag-doped ZnMgO thin films are varied depending on the substrate temperature, as shown in Fig. 1(b). It can be seen that the position of the (0 0 2) peak first shifts to a lower angle consistently and then recovers to a higher angle slightly as increasing the substrate temperature from 300 to 500 °C. As is well known, Ag in ZnO can act as an amphoteric dopant, existing both on substitutional Zn sites and in the interstitial sites. The quasichemical reaction for Ag in ZnMgO thin films may be described as follows [19]:

$$Ag_2O \rightarrow Ag'_{Zn} + Ag_i^{\bullet} + O_O, \quad (1)$$

where Ag'_{Zn} is Ag at a Zn site, $Ag_i^{\bullet}$ is Ag at an interstitial site and O_O is O at an oxygen site. Therefore, the initial decrease of the (0 0 2) peak position is ascribed to the increase of the number of substitutional Ag^+ ion on the Zn^{2+} lattice sites with the increase of substrate temperature, which expands the lattice parameter due to the radius of Ag^+ ion (1.02 Å) is larger than that of Zn^{2+} ion (0.60 Å) [20]. On the other hand, the partial formation of Ag interstitials at higher temperature may increase the ZnO lattice and then cause the lower angle shifting of the (0 0 2) peak. In addition, it can be observed from Fig. 1(b) that the lattice parameter of c-axis has been estimated in the range from 5.194 to 5.201 Å, which is smaller than the value of 5.207 Å for bulk ZnO. This is ascribed to the smaller ionic radius of Mg^{2+} (0.57 Å) than Zn^{2+} (0.60 Å) [20]. According to the above analysis, it can be inferred that the Ag-doped ZnMgO film prepared at 400 °C has the best crystal quality owing to the coordination of Mg^{2+} and Ag^+ in the film.

Table 1 summarizes the electrical properties of Ag-doped ZnMgO films measured by Hall-effect measurements in the van der Pauw configuration [21]. The quartz substrates used here can assure that the conducting features of the films are not affected by the substrate and are completely attributed to Ag-doped ZnMgO thin films. It can be seen that the electrical properties of the films are strongly influenced by the substrate temperature during the film growth. When the substrate temperature is low (300 °C), the film possesses relatively high resistivity and exhibits n-type conduction. This may be caused by the fact that the amount of Ag_{Zn} acceptor in the film grown at such temperature is insufficient to compensate the intrinsic donor defects such as V_O and Zn_i. As a result, the film exhibited n-type conduction. As the substrate temperature increases, the p-type conduction of the films is confirmed and enhanced due to the Ag atoms are activated gradually. The optimized result with a resistivity of 24.96 Ω cm, a Hall mobility of 0.32 $cm^2 V^{-1} s^{-1}$, and a hole concentration of 7.89×10^{17} cm^{-3}, is realized at the substrate temperature of 400 °C. The realization of p-type conduction indicates the formation of Ag_{Zn} acceptors in the film. As the substrate temperature further increases, weak p-type conduction is found with high resistivity and low carrier concentration. It is inferred that the degradation in electrical properties may be associated with the partial formation of Ag interstitials at higher temperature which is harmful to p-type doping, as supported by the XRD results. Besides, the reevaporation of few Ag accepters at high substrate temperature would be another possible reason for the deterioration in electrical properties. Similar behaviors have been observed for p-type Li-doped ZnMgO thin films by Pan et al. [22]. Therefore, it is reasonable to speculate that Ag atoms substitute for Zn atoms acting as effective acceptors in Ag-doped ZnMgO thin films.

In order to investigate the element composition distribution in the Ag-doped ZnMgO thin film, the depth profile of the main elements in the film is carried out by SIMS measurement, as presented in Fig. 2. It is evident that Ag has been clearly detected, and its

Table 1
Electrical properties of Ag-doped ZnMgO thin films deposited at different substrate temperatures.

Sample	Substrate temperature (°C)	Resistivity (Ω cm)	Hall mobility ($cm^2 V^{-1} s^{-1}$)	Carrier concentration (cm^{-3})	Carrier type
S1	300	3.25×10^4	3.05	6.30×10^{13}	n
S2	350	2812	0.40	5.53×10^{15}	p
S3	400	24.96	0.32	7.89×10^{17}	p
S4	450	693.4	0.45	1.98×10^{16}	p
S5	500	3887	0.56	2.85×10^{15}	p

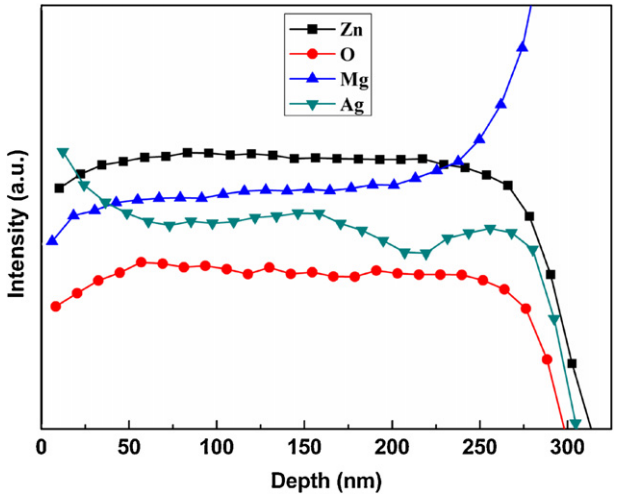

Fig. 2. SIMS depth profile of Ag-doped ZnMgO thin film deposited at 400 °C.

concentration profile is found to be relatively uniform from the surface to the interface. This indicates that the Ag has been incorporated into the ZnMgO film, which is responsible for the p-type conduction. However, no quantitative results could be obtained due to the lack of reference samples for the SIMS measurement. In addition, the film thickness can be estimated from the SIMS profile curve to be about 280 nm, which is in good agreement with the result obtained by SEM measurement.

To identify the chemical bonding states of Ag in the Ag-doped ZnMgO thin films, the XPS measurement is carried out. Fig. 3 provides the XPS spectrum of Ag 3d core levels of the film grown at 400 °C and the results have been calibrated according to the C 1s peak at ~285 eV. The concentration of Ag in the film is calculated to be 1.17 at%, agreeing well with that in the target. In Fig. 3, a peak located at 367.45 eV is observed, which is characteristic of the chemical state of Ag element. It is reported that the binding energy of Ag $3d_{5/2}$ is in the range from 368.1 to 368.4 eV for Ag^0 and from 367.4 to 367.8 eV for Ag^+ ions, respectively [23,24]. Therefore, the 367.45 eV peak can be assigned to Ag_{Zn}–O bonds, indicating that Ag may principally occupy Zn sites in the state of Ag^+ ions in the Ag-doped ZnMgO film and act as acceptors.

Fig. 4 presents the room-temperature PL spectra of the Ag-doped ZnMgO thin films as a function of substrate temperature. All the films exhibit an intense emission peak in UV region and a broad emission band in visible region. The peaks centered at about 358 nm are attributed to the excitonic near-band-edge (NBE) emission. It is found that the intensity of the narrow NBE emission peaks becomes more intense and sharper with increasing substrate temperature, reaches a maximum value at 400 °C, and then decreases gradually as the substrate temperature further increases. However, the intensity of the broad green (GB) emission peaks centered at 550 nm first decreases and then increases with increasing substrate temperature, as clearly seen in Fig. 4. It is well known that such broad deep level emission is closely related to the intrinsic defects, such as Zn interstitial (Zn_i), oxygen vacancy (V_O) and Zn antisite (O_{Zn}), which are believed to act as donor defects [25,26]. According to the above analysis, we deduce that suitable substrate temperature will be helpful in the suppression of oxygen-related defects and be more favorable for the formation of p-type conduction. Note that the film grown at 400 °C shows the strongest NBE emission and weakest GB emission, suggesting the optimized p-type conduction can be obtained at such temperature. The results are consistent with the XRD and Hall measurements.

To verify the p-type conduction of the Ag-doped ZnMgO thin films we obtained, a p-i-n structured heterojunction combining with an intrinsic ZnO buffer layer was made by layer-by-layer growth, and the schematic illustration of the p-i-n junction is shown in the bottom right inset in Fig. 5. The electron concentrations in the n-type Al-doped ZnMgO layer and undoped intrinsic ZnO (i-ZnO) layer are approximately 9.77×10^{17} cm^{-3} and 4.47×10^{15} cm^{-3}, respectively. After that, Ag-doped p-ZnMgO film was grown on the i-ZnO layer. The thicknesses of the three

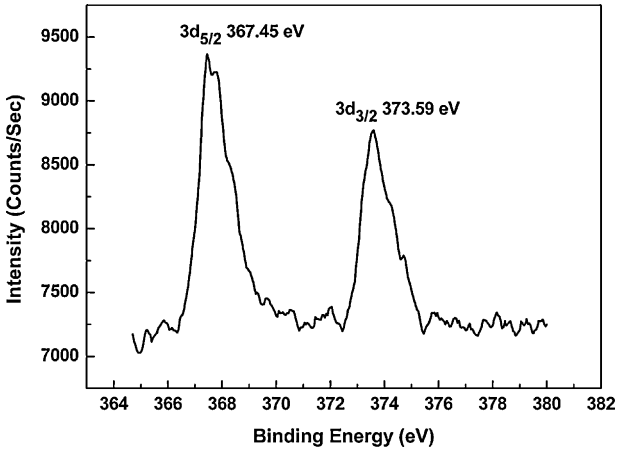

Fig. 3. XPS spectrum of Ag 3d core levels of the Ag-doped ZnMgO thin film grown at 400 °C.

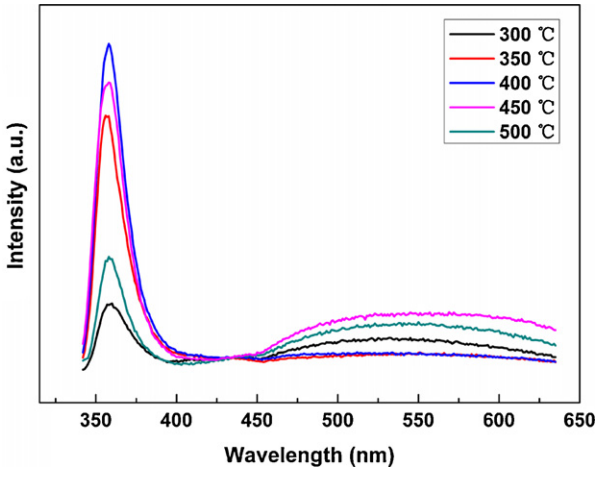

Fig. 4. Room-temperature PL spectra of Ag-doped ZnMgO thin films deposited at different substrate temperatures.

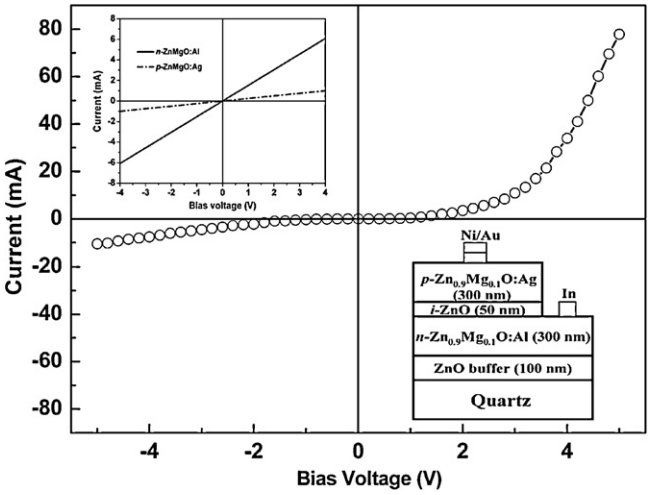

Fig. 5. *I–V* characteristics of a p-i-n structured Ag-doped ZnMgO/i-ZnO/Al-doped ZnMgO heterojunction. The insets show their schematic diagram and the *I–V* curves of the Ni/Au contact to the p-type Ag-doped ZnMgO layer and the In contact to the n-type Al-doped ZnMgO layer.

layers are 300, 50, and 300 nm, respectively. Au/Ni and indium metal were deposited onto the p-type Ag-doped ZnMgO layer and n-type Al-doped ZnMgO layer, respectively, acting as electrodes. The *I–V* curve of the structure is shown in Fig. 5. Obvious rectifying behaviors with a turn-on voltage of approximately 3 V are observed from the curve. Note that both the *I–V* curves of the contacts on the p-type and n-type layers are beelines, as shown in the upper left inset of Fig. 5, revealing that both electrodes on n-type and p-type ZnO layers are ohmic contacts. The above facts indicate that the rectifying behavior observed in the *I–V* curve of the p-i-n structured heterojunction originates from the junction instead of the Schottky contacts [27,28].

4. Conclusions

In summary, p-type Ag-doped ZnMgO thin films had been prepared on quartz substrates by pulsed laser deposition in oxygen ambient using the sintered ZnO target containing 10 at% MgO and 0.5 at% Ag_2O. The film prepared at 400 °C had the best crystal quality and showed p-type conduction with a resistivity of 24.96 Ω cm, a Hall mobility of 0.32 $cm^2 V^{-1} s^{-1}$, and a hole concentration of 7.89×10^{17} cm^{-3} at room temperature. SIMS and XPS measurements showed that Ag had been incorporated in to the films and principally occupied Zn sites in the state of Ag^+ ions. The formation of good p-type conduction in this film is closely related to the increase of substitutional-Ag (Ag_{Zn}) density and the suppression of the oxygen-related defects. A heterojunction based on Ag-doped ZnMgO/i-ZnO/Al-doped ZnMgO showed obvious rectifying behaviors with a turn-on voltage of approximately 3 V. These results will represent meaning steps for ZnO/ZnMgO superlattices, quantum wells, and UV optoelectronic devices.

Acknowledgements

This work is supported by National Natural Science Foundation of China No. 51072181, Doctorate Fund of the Ministry of Education No. 20090101110044.

References

[1] L. Balakrishnan, S. Gowrishankar, P. Premchander, N. Gopalakrishnan, J. Alloys Compd. 512 (2012) 235.
[2] D.C. Look, B. Claflin, Phys. Stat. Sol. b 241 (2004) 624.
[3] J. Zeng, S. Wang, P. Tao, J.C. Xu, J. Alloys Compd. 476 (2009) 60.
[4] H. Long, G.J. Fang, H.H. Huang, X.M. Mo, W. Xia, B.Z. Dong, X.Q. Meng, X.Z. Zhao, Appl. Phys. Lett. 95 (2009) 013509.
[5] P.L. Chen, X.Y. Ma, D.S. Li, Y.Y. Zhang, D.R. Yang, Appl. Phys. Lett. 90 (2007) 251115.
[6] X.Q. Gu, L.P. Zhu, Z.Z. Ye, Q.B. Ma, H.P. He, Y.Z. Zhang, B.H. Zhao, Sol. Energy Mater. Sol. Cells 92 (2008) 343.
[7] S.B. Zhang, S.H. Wei, A. Zunger, Phys. Lett. B 63 (2001) 075205.
[8] S. Aksoy, Y. Caglar, S. Ilican, M. Caglar, J. Alloys Compd. 512 (2012) 171.
[9] Y. Xue, H.P. He, Y.Z. Jin, Z.Z. Ye, Appl. Surf. Sci. 257 (2011) 5927.
[10] W.W. Liu, B. Yao, Y.F. Li, B.H. Li, Z.Z. Zhang, C.X. Shan, J.Y. Zhang, D.Z. Shen, X.W. Fan, J. Alloys Compd. 504 (2010) 484.
[11] Y.J. Li, Y.W. Heo, Y. Kwon, K. Ip, S.J. Pearton, D.P. Norton, Appl. Phys. Lett. 87 (2005) 072101.
[12] X. Dong, Y.B. Liu, K.K. Huang, W. Zhao, Y. Ye, X.C. Xia, Y.T. Zhang, J. Wang, B.L. Zhang, G.T. Du, J. Phys. D: Appl. Phys. 42 (2009) 235101.
[13] P. Wang, N.F. Chen, Z.G. Yin, R.X. Dai, Y.M. Bai, Appl. Phys. Lett. 89 (2006) 202102.
[14] X. Zhang, X.M. Li, T.L. Chen, C.Y. Zhang, W.D. Yu, Appl. Phys. Lett. 87 (2005) 092101.
[15] L.Q. Zhang, Z.Z. Ye, J.Y. Huang, B. Lu, H.P. He, J.G. Lu, Y.Z. Zhang, J. Jiang, J. Zhang, K.W. Wu, W.G. Zhang, J. Alloys Compd. 509 (2011) 7405.
[16] L. Gong, Z.Z. Ye, J.G. Lu, Vacuum 85 (2010) 365.
[17] O. Volnianska, P. Boguslawski, J. Kaczkowski, P. Jakubas, A. Jezierski, E. Kaminska, Phys. Rev. B 80 (2009) 245212.
[18] L.J. Sun, J. Hu, H.Y. He, X.P. Wu, X.Q. Xu, B.X. Lin, Z.X. Fu, B.C. Pan, Solid State Commun. 149 (2009) 1663.
[19] H.S. Kang, B.D. Ahn, J.H. Kim, G.H. Kim, S.H. Lim, H.W. Chang, S.Y. Lee, Appl. Phys. Lett. 88 (2006) 202108.
[20] R.D. Shannon, Acta Crystallogr. A 32 (1975) 751.
[21] Q. Wan, Appl. Phys. Lett. 89 (2006) 176103.
[22] X.H. Pan, Z.Z. Ye, J.Y. Huang, Y.J. Zeng, H.P. He, X.Q. Gu, L.P. Zhu, B.H. Zhao, J. Cryst. Growth 310 (2008) 1029.
[23] R. Deng, B. Yao, Y.F. Li, T. Yang, B.H. Li, Z.Z. Zhang, C.X. Shan, J.Y. Zhang, D.Z. Shen, J. Cryst. Growth 312 (2010) 1813.
[24] R.Q. Chen, C.W. Zou, J.M. Bian, A. Sandhu, W. Gao, Nanotechnology 22 (2011) 105706.
[25] T. Prasada Rao, M.C. Santhosh Kumar, J. Alloys Compd. 509 (2011) 8676.
[26] M.A. Thomas, J.B. Cui, J. Appl. Phys. 105 (2009) 093533.
[27] F.J. Lugo, H.S. Kim, S.J. Pearton, C.R. Abernathy, B.P. Gila, D.P. Norton, Y.L. Wang, F. Ren, Electrochem. Solid State Lett. 12 (2009) H188.
[28] F. Sun, C.X. Shan, B.H. Li, Z.Z. Zhang, D.Z. Shen, Z.Y. Zhang, D. Fan, Opt. Lett. 36 (2011) 499.